Validity of solid-state Li⁺ diffusion coefficient estimation by electrochemical approaches for lithium-ion batteries

Downloaded from: https://research.chalmers.se, 2026-09-10 06:46 UTC

Citation for the original published paper (version of record):
Geng, Z., Chien, Y., Lacey, M. et al (2022). Validity of solid-state Li⁺ diffusion coefficient estimation by electrochemical
approaches for lithium-ion batteries. Electrochimica Acta, 404.
http://dx.doi.org/10.1016/j.electacta.2021.139727

N.B. When citing this work, cite the original published paper.

research.chalmers.se offers the possibility of retrieving research publications produced at Chalmers University of Technology. It covers all kind of research output: articles, dissertations, conference papers, reports etc. since 2004. research.chalmers.se is administrated and maintained by Chalmers Library

(article starts on next page)

Electrochimica Acta 404 (2022) 139727

Contents lists available at ScienceDirect

Electrochimica Acta

journal homepage: www.elsevier.com/locate/electacta

Validity of solid-state Li^+ diffusion coefficient estimation by electrochemical approaches for lithium-ion batteries

Zeyang Geng[a,*], Yu-Chuan Chien[b], Matthew J. Lacey[c], Torbjörn Thiringer[a], Daniel Brandell[b]

[a] Department of Electrical Engineering, Division of Electric Power Engineering, Chalmers University of Technology, SE-412 96 Göteborg, Sweden
[b] Department of Chemistry - Ångstrm Laboratory, Uppsala University, SE-751 21 Uppsala, Sweden
[c] Scania CV AB, SE-15187 Södertlje, Sweden

ARTICLE INFO

Article history:
Received 14 October 2021
Revised 3 December 2021
Accepted 7 December 2021
Available online 14 December 2021

Keywords:
Li-ion battery
Modelling
Galvanostatic intermittent titration technique
Intermittent current interruption

ABSTRACT

The solid-state diffusion coefficient of the electrode active material is one of the key parameters in lithium-ion battery modelling. Conventionally, this diffusion coefficient is estimated through the galvanostatic intermittent titration technique (GITT). In this work, the validity of GITT and a faster alternative technique, intermittent current interruption (ICI), are investigated regarding their effectiveness through a black-box testing approach. A Doyle-Fuller-Newman model with parameters for a $LiNi_{0.8}Mn_{0.1}Co_{0.1}O_2$ electrode is used as a fairly faithful representation as a real battery system, and the GITT and ICI experiments are simulated to extract the diffusion coefficient. With the parameters used in this work, the results show that both the GITT and ICI methods can identify the solid-state diffusion coefficient very well compared to the value used as input into the simulation model. The ICI method allows more frequent measurement but the experiment time is 85% less than what takes to perform a GITT test. Different fitting approaches and fitting length affected the estimation accuracy, however not significantly. Moreover, a thinner electrode, a higher C-rate and a greater electrolyte diffusion coefficient will lead to an estimation of a higher solid-state diffusion coefficient, generally closer to the target value.

© 2021 The Author(s). Published by Elsevier Ltd.
This is an open access article under the CC BY license (http://creativecommons.org/licenses/by/4.0/)

1. Introduction

A lithium (Li) ion battery is a complicated electrochemical system and its performance is dependent on a multitude of material properties, among which the solid-state diffusion coefficient D_s of Li^+ is one of the key parameters, since the mass transport in these particles is the rate-limiting processes for thin electrodes, and the corresponding resistances constitute a major part of the total battery overpotential. The value of D_s is, however, not straightforwardly obtained, which is a major obstacle for more precise battery modelling. While the diffusion coefficient can be theoretically estimated from density functional theory (DFT) [1,2] or Molecular Dynamics (MD) simulations [3,4], it is more frequently experimentally determined by electrochemical approaches, including the galvanostatic intermittent titration technique (GITT), potentiostatic intermittent titration technique (PITT), electrochemical impedance spectroscopy (EIS) and cyclic voltammetry (CV) [5]. Of these, GITT is arguably the most popular choice due to its comparative robustness, while still being time-consuming.

GITT was original proposed by Weppner and Huggins [6] for a Li_3Sb electrode, and then later generalized for porous insertion electrode materials used in lithium-ion batteries [7–9]. In the GITT test, a current pulse is applied when the cell is in an equilibrium state and the voltage response follows a linear relationship with the square root of time. The diffusion coefficient can thus be calculated from the voltage response, assuming that the particle size is known. Normally the current pulses are applied at different states of charge (SOC) as the solid-state diffusion coefficient is a SOC dependent parameter. Since an equilibrium initial condition is required before the current pulse, a long relaxation time is needed in between each SOC level, which makes the GITT method very time consuming. In recent years, however, the alternative intermittent current interruption (ICI) technique has been proposed [10] as a faster alternative to GITT [11]. Using ICI, the voltage response during a current interruption is monitored, which also follows a linear relationship with the square root of time. Since the ICI method does not require the cell to be in an equilibrium state, the most time consuming part in the GITT method, i.e. the relaxation period, can thus be omitted.

Employing the same experimental object and setup, different methods can sometimes provide fairly similar results for the solid

* Corresponding author.
E-mail address: zeyang.geng@chalmers.se (Z. Geng).

https://doi.org/10.1016/j.electacta.2021.139727
0013-4686/© 2021 The Author(s). Published by Elsevier Ltd. This is an open access article under the CC BY license (http://creativecommons.org/licenses/by/4.0/)

Nomenclature

T	Temperature, K
n	Number of electrons involved in the redox reaction
F	Faraday constant, 96485 s·A/mol
i	Current density per electrode area, A/m^2
j_0	Exchange current density, A/m^2
α	Transfer coefficient
η	Overpotential caused by the redox reaction, V
c	Lithium ion concentration, mol/m^3
$c_{s,surf}$	Lithium ion concentration on the particle surface, mol/m^3
k	Reaction rate constant
$c_{s,\max}$	Maximum concentration in the intercalation material, mol/m^3
c_0	Initial concentration in the intercalation material, mol/m^3
t	Time, s
j	Charge transfer current density per surface area, A/m^2
ϵ	Volume fraction
D	Diffusion coefficient, m^2/s
t_+^0	Transference number of lithium ion
κ	Electrolyte conductivity, S/m
L	Electrode thickness, m
r_s	Radius of solid particles, m
r	Radial distance in the particle, m
I	Given current density, A/m^2
E	Terminal voltage, V
f_A	Activity dependence
x	Stoichiometry, $x = c_s/c_{s,\max}$
λ	Positive roots of $\lambda = \tan(\lambda)$
s	Solid phase
l	Liquid phase
a	Anodic
c	Cathodic
0	Initial condition

state Li^+ diffusion coefficient D_s. For example, Chien et al. obtained diffusion coefficient values with the GITT and ICI methods with an excellent agreement with each other [11], and a similar comparison has been made between the GITT and EIS methods displaying a good match [12]. Nevertheless, the reported D_s values from different literature of one specific material often vary within several orders of magnitude and this fact makes it challenging to decide a proper value to use in battery modelling. The reason for this large spread of the reported D_s values can be explained by the differences in the electrode design, electrolyte composition, current magnitude, fitting method, resting period, etc. Moreover, the validity of GITT, as well as other techniques employed for this purpose, is being questioned and discussed as the underlying assumptions are not completely valid when they are applied for porous insertion lithium-ion electrodes [13,14]. Dees et al. has shown that the D_s value estimated with the GITT theory is generally lower that the value used in their DC electrochemical model [9].

In principle, determining the 'true' solid state Li^+ diffusion coefficient of an electrode material through electrochemical measurements on battery cells is associated with large challenges, due to the inherent complexity of the system and the abundance of other simultaneous processes taking place. Moreover, the D_s value is dependent on several inherent materials properties, e.g. particle shape and grain boundaries. Therefore, to consistently and precisely validate the electrochemical approaches for estimating the solid-state Li^+ diffusion coefficient of a battery material in a porous electrode is difficult experimentally. Nevertheless, the counterparts to these methods in detailed continuum models of Li-ion batteries are equally valid as the experimental approaches. The philosophy in this work is that, if experiments are designed according to well-established electrochemical methods, and then emulated in simulations with a fully known battery cell model, using results from simulations one should be able to extract the same solid-state diffusion coefficient as what was put in the model, as a proof of the method validity. Alternatively, if the solid-state diffusion coefficient found from the simulation results would differ from that put into the model, the reasons should be analyzed and the deviation shall be quantified, since it is essential to know to what extent these electrochemical methods can be trusted to parameterize accurate models.

Therefore, a theoretical validation is demonstrated in this work for the GITT and ICI method when applying them for a porous electrode. The classical Doyle-Fuller-Newman (DFN) model [15,16] is one of the most commonly employed continuum models for simulating lithium-ion batteries and it is considered to be a fairly faithful representation of a real battery system. In this work, a DFN model previously implemented in MATLAB [17] with parameters from Chen et al. [7] for $LiNi_{0.8}Mn_{0.1}Co_{0.1}O_2$ is used for black-box testing. The input is current sequences designed according to the GITT and ICI methods and the output is the battery terminal voltage which is used to estimate the solid-state diffusion coefficient. The advantage is that after the black-box testing, different physical phenomenon in the model can be studied in details to demonstrate the origins for any deviations between the estimated D_s value and the true value used in the model. The main purpose of the study is thus to reveal how the porous electrode structure will affect the solid-state diffusion coefficient estimation when employing the GITT and ICI methods, which was originally proposed for a more uniform electrode material. This work also demonstrates the impact on the D_s estimation accuracy with different fitting methods, fitting lengths, current magnitude, electrode thickness as well as electrolyte properties.

2. Theory

Following the DFN model, the mass transport process in the electrode particles is modelled by Fick's law in a spherical coordinate system

$$\frac{\partial c_s}{\partial t} = D_s\left(\frac{\partial^2 c_s}{\partial r^2} + \frac{2}{r}\frac{\partial c_s}{\partial r}\right) \tag{1}$$

where c_s is the lithium-ion concentration in the solid active material, t is the time, D_s is the solid-state diffusion coefficient of lithium ions, and r is the distance from the particle center. When the cell is in an equilibrium state

$$c_s|_{t=0} = c_0 \tag{2}$$

If a constant current j is applied to the surface of a particle at $t =$ 0 s, then the lithium ion flux at the surface is

$$\frac{\partial c_s}{\partial r}|_{r=r_s} = -j/(FD_s) \tag{3}$$

where F is the Faraday constant. The symmetric shape of the particle fulfills the condition

$$\frac{\partial c_s}{\partial r}|_{r=0} = 0 \tag{4}$$

The analytical solution of (1) with the boundary conditions in (2)–(4) is

$$c_{s,surf} = c_0 + \frac{jr_s}{FD_s} f\left(\frac{D_s t}{r_s^2}\right) \tag{5}$$

$$f(\frac{D_s t}{r_s^2}) = f(\tau) = 3\tau + 0.2 - 2\sum_{n=1}^{\infty}\frac{1}{\lambda_n^2}\exp(-\lambda_n^2\tau) \tag{6}$$

where λ_n is the positive roots of $\lambda = \tan(\lambda)$ [8]. The expression in (6) can be approximated to be

$$f(\tau) = \begin{cases} \frac{2}{\sqrt{\pi}}\sqrt{\tau} & \tau \ll 1 \\ 3\tau + 0.2 & \tau \gg 1 \end{cases} \tag{7}$$

According to the mathematical description above, the diffusion coefficient D_s could be found from the step response of c_s. In most cases, the concentration is very difficult to measure directly, therefore the terminal voltage E - the experimentally easily measurable parameter - is used instead. The step response (5) is therefore rewritten as

$$E = E_0 + \frac{dE}{dc}\frac{jr_s}{FD_s}f(\frac{D_s t}{r_s^2}) \tag{8}$$

In (8), dE/dc is often assumed to be a constant within a small SOC interval, i.e. the voltage profile is linear

$$\frac{dE}{dc} = \lim_{\Delta c\to 0}\frac{\Delta E}{\Delta c} = \frac{\Delta E_{GITT}}{It_{pulse}/(FL\epsilon_s)} \tag{9}$$

where I is the current density on the electrode, t_{pulse} is the time length of the current pulse, L is the electrode length, ϵ_s is the volume fraction of the solid, and ΔE_{GITT} is the voltage difference between two equilibrium states before and after the current pulse. Furthermore, the local current density on particle j in (8) is $j = I/(S_a L)$, where $S_a = 3\epsilon_s/r_s$ is the specific surface area. Combining (8) and (9) gives

$$E = E_0 + \frac{\Delta E_{GITT}}{t_{pulse}}\frac{r_s^2}{3D_s}f(\frac{D_s t}{r_s^2}) \tag{10}$$

When $\tau = D_s t/r_s^2 \ll 1$, (10) can be approximated as

$$E = E_0 + \frac{2}{3}\frac{\Delta E_{GITT}}{t_{pulse}}\frac{r_s\sqrt{t}}{\sqrt{\pi D_s}} \tag{11}$$

and thus the diffusion constant can be found to be

$$D_s = \frac{4}{9\pi}(\frac{r_s}{dE/d\sqrt{t}}\frac{\Delta E_{GITT}}{t_{pulse}})^2 \tag{12}$$

The approach in (12) is one of the most commonly used fitting methods employed for GITT, and typically only a chosen region of the voltage step response is used to fit $dE/d\sqrt{t}$ to fulfill the approximation condition $\tau \ll 1$. The validity of this approximation is demonstrated in Fig. 1. It can be observed that the system response follows a linear relationship with $\sqrt{\tau}$ in the beginning and this approximation is considered to be valid when $\tau < 0.0032$ [11]. The time axis is shown for two sets of parameters reported for $LiNi_{0.8}Mn_{0.1}Co_{0.1}O_2$: $r_s = 5.22$ μm, $D_s = 1.48\times10^{-15}$ m^2/s [7] and $r_s = 3.8$ μm, $D_s = 5\times10^{-13}$m^2/s [18]. In the first case, $\tau < 0.0032$ corresponds to $t = \tau r_s^2/D_s < 58.92$ s and therefore the voltage response within this time length can be used to fit $dE/d\sqrt{t}$ in (12) for the diffusion coefficient identification. In contrast, the condition $\tau < 0.0032$ corresponds to $t < 0.09$ s in the latter case, meaning that the $\tau \ll 1$ approximation fails to describe the system response almost instantly. For such material properties, the expression in (10) can be used instead, which is not limited by the time constant of the system [19]. In this work, both of the two methods will be examined. Moreover, it should be acknowledged that there exist other less common variants to estimate the dE/dc in (8), resulting in similar expressions as those described above [8,20,21], but those variants will not be further discussed here.

In the GITT method, the solution of voltage response in (8) is solved with the initial condition where the cell is in an equilibrium state, meaning that a sufficient relaxation time period needs

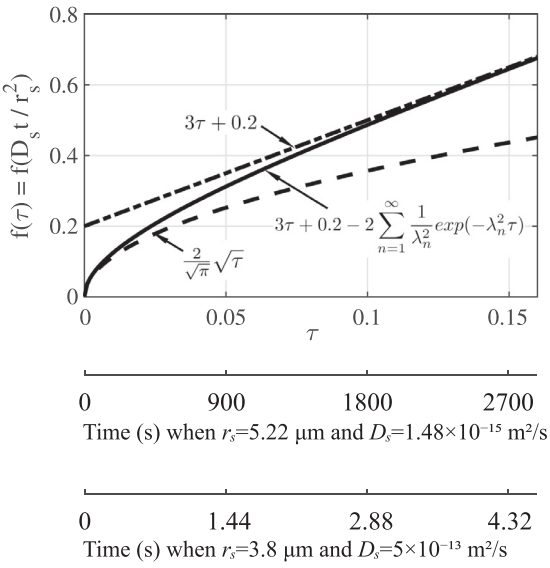

Fig. 1. The function in (6) is plotted as a solid line (n = 1272 for λ_n), while its approximations in (7) are plotted as dashed lines.

to take place between the current pulses. This generally very long time consumption has been considered to be the main disadvantage of GITT when compared with other methods. Alternatively, the more efficient ICI technique [10] can be considered as a possible replacement. In ICI, the step response when the current is switched off is utilized. When the current is stopped at $t = t_0$, the concentration on the surface is

$$c_{s,surf} = c_0 + \frac{jr_s}{FD_s}f(\frac{D_s t}{r_s^2}) - H(t)\frac{jr_s}{FD_s}f(\frac{D_s(t-t_0)}{r_s^2}) \tag{13}$$

$$H(t) = \begin{cases} 0 & t < t_0 \\ 1 & t \geq t_0 \end{cases} \tag{14}$$

where t is counted from the time when the current is switched on [11]. Similar as in the GITT method, the initial concentration response when the current stops also follows a linear relationship with $\sqrt{t}$ according to the approximation in (7). In principle, the diffusion coefficient D_s could be derived in a similar manner as in (12), resulting in the expression

$$D_s = \frac{4}{9\pi}(\frac{r_s}{dE/d\sqrt{t}}\frac{\Delta E_{ICI}}{\Delta t})^2 \tag{15}$$

where $dE/d\sqrt{t}$ is fitted during the zero current period and $\Delta E_{ICI}/\Delta t$ is estimated from a pseudo open circuit voltage, which is obtained by subtracting the IR drop from the voltage curve, as shown in Fig. 2. Moreover, the ICI method does not require an equilibrium initial condition as in the GITT method, and the cell can instead be in a dynamic state under a constant current before the current interruption. This feature renders the ICI method considerably less time consuming.

It should be acknowledged that the derivation above is based the following assumptions:

- Fick's law is applied.
- The particle has a spherical shape and the diffusion is symmetric.
- The voltage profile is linear during a short interval, i.e. dE/dc is a constant.
- The current density at the particle surface is constant.
- The over-potential caused by other electrochemical processes can be ignored.

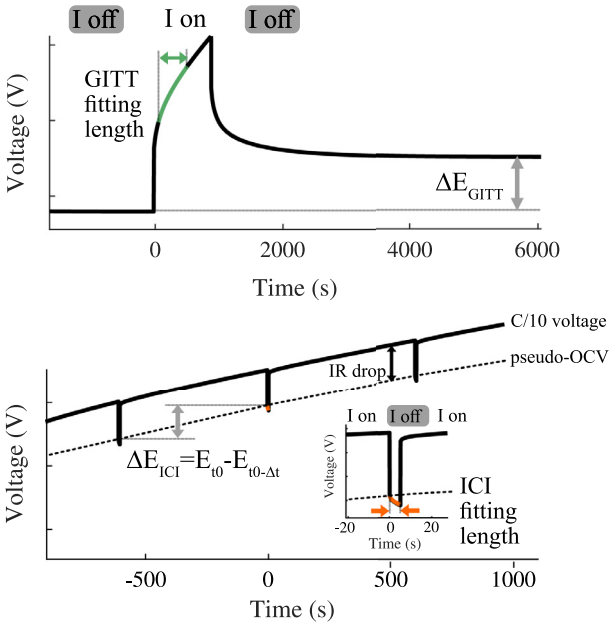

Fig. 2. The voltage response during one current pulse, comparing the GITT (above) and ICI (below) approaches. In the ICI approach, t_0 is the time when the current is interrupted in the region of interest, and Δt is the time interval between two current interruptions.

The first two assumptions are the same as in the general DFN model, and their impact is thus not examined. The impact of the latter three assumptions will be studied hereafter to verify the validity of the GITT and ICI methods when they are applied for a porous lithium ion electrode.

3. Simulation setup

The mathematical model is a DFN model implemented in MATLAB as described in [17] and the parameters are from Chen et al. [7], listed in Table 1. Two values are here adjusted from the original values reported in [7]; one is the electronic conductivity of the electrode material and the other is the reaction rate constant in the charge transfer reaction. The electronic conductivity of $LiNi_{0.8}Mn_{0.1}Co_{0.1}O_2$ (NMC811) is reported to be 0.18 S/m in [7]. However, conductive carbon additives are often added in cell manufacturing to improve the conductivity of the electrode. Therefore, a higher value 10 S/m is used in this work to be closer to reality. The other parameter, the reaction rate constant in the charge transfer reaction, is reduced to increase the charge transfer resistance and thus improve the stability of the system. Instability issues appear under a certain parameter combination with solvers used in [17] but can be overcome by slightly adjusting the parameters. This adjustment is considered to not affect the conclusions in this study for the solid-state diffusion coefficient identification. The value of the target parameter D_s is 1.48×10^{-15} m^2/s which was experimentally determined by GITT in [7]. This value is the input of the model and will be used as the reference to compare with the D_s values obtained from the GITT and ICI simulations.

A symmetric cell setup is employed: NMC811 ($x_0 = x_{min}$) - separator - NMC811 ($x_0 = x_{max}$). When the cell is charged, one electrode NMC811 ($x_0 = x_{min}$) is being lithiated while the other electrode NMC811 ($x_0 = x_{max}$) is being delithiated. For a positive electrode material, x_{min} and x_{max} correspond to 100% and 0% SOC respectively. These two stoichiometry limits were obtained from the half-cell data in [7]. This setup has the advantage that the lithiation and delithiation processes of one electrode material can be simulated within one simulation, thereby saving computational time. The electrolyte potential in the middle of the separator is used as the reference potential (ground) to mimic a three-electrode cell. The DFN model is a pseudo two-dimensional (P2D) model where one dimension is in the cross-section direction of the cell to address the current distribution in the electrodes, and the electrolyte concentration distribution through the electrodes and the separator, while another dimension is in the radius direction of the particles for the solid-state diffusion processes. Both dimensions are evenly meshed, with 10 mesh elements in each electrode and the separator and 100 mesh elements in each particle. The time step is 0.1 s during the region used for fitting, and 5 s for the rest to shorten the simulation time.

$$\begin{aligned} OCV(x) = & -0.8090x + 4.4875 - 0.0428 \\ & \times \tanh(18.5138(x - 0.5542)) - 17.7326 \\ & \times \tanh(15.789(x - 0.3117)) \\ & + 17.5842 \times \tanh(15.9308(x - 0.312)) \end{aligned} \quad (16)$$

The applied current is 0.1 C = 0.498 mA/cm^2 for both the GITT and ICI simulations. In the GITT simulation, the current pulse is 900 s with 1.5 h of relaxation in between. In reality, lithium-ion cells take longer time to reach equilibrium again after the pulse, but 1.5 h is sufficient in these simulations. For the ICI procedure, the current is interrupted for 5 s every 5 min.

Three identification approaches are used to identify the diffusion coefficient D_s

- GITT full expression fitting according to (10)
- GITT $\tau \ll 1$ approximation fitting according to (12)
- ICI fitting according to (15)

In (12) and (15), $dE/d\sqrt{(t)}$ is fitted within a selected region, as shown in Fig. 2. The starting point of the fitting region is one second after the current is switched in order to avoid the transient period of other electrochemical processes. In reality, this can be adjusted to a later point in time to exclude the effect of double layer capacitance. Different fitting lengths are used in the data processing. With the full expression fitting in (10), the fitting length is unlimited. However, with the $\tau = D_s t / r_s^2 \ll 1$ fitting in (12) and (15), the fitting length should not be too long to diverge from the conditions of approximation.

4. Results and discussions

4.1. D_s estimation through GITT and ICI methods

The simulated voltage profiles during the GITT and ICI tests are shown in Fig. 3, which resemble the experimental results reported in literature [9,11]. With the symmetric cell setup described in the previous section, the delithiation and lithiation processes are simulated simultaneously. In the GITT test, the voltage step response is clearly visible under a C/10 current pulse and in total 35 current pulses are applied through the entire SOC range. With the simulation protocol, i.e. 15 min pulse with 1.5 h relaxation, the time required to complete a GITT test in a real experiment will be 63 h. On the other hand, 53 current interruptions take place in the ICI test, with the corresponding experiment time being merely 9 h. The ICI method thereby allows more identification occasions for the diffusion coefficient, with less than 15% of the time it takes to complete a GITT measurement.

The derived diffusion coefficient D_s is presented in Fig. 4a. In the GITT method, the voltage response between $t = 1$ s and $t = 21$ s (the current is applied at $t = 0$ s) is used to for the fitting in (12), and the voltage response between $t = 1$ s and $t = 5$ s (the current is interrupted at $t = 0$ s) is used in the ICI method to fit with the expression in (15). The diffusion coefficient used in the model is 1.48×10^{-15} m^2/s [7] and it is plotted as the 'true value'

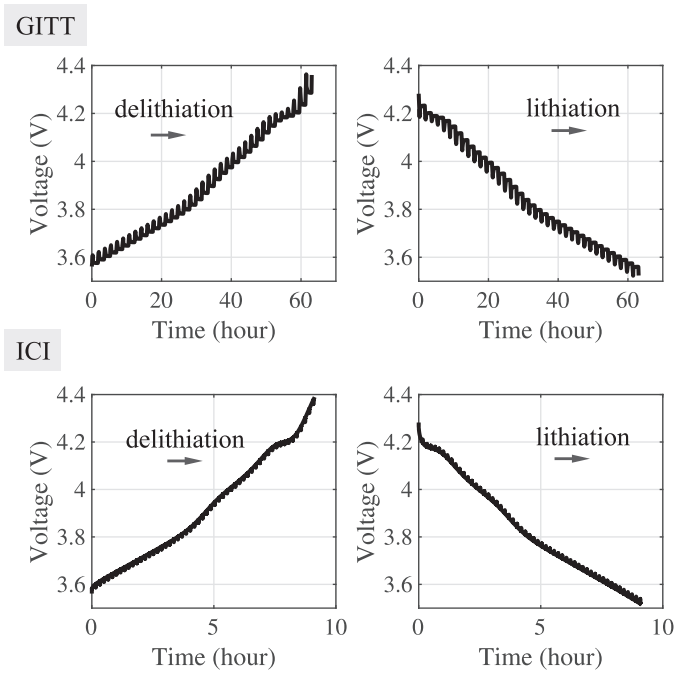

Fig. 3. Simulated voltage profiles of an NMC811 electrode during lithiation and delithiation processes with GITT and ICI methods.

in Fig. 4a. Although in reality the diffusion coefficient of lithium ions is SOC dependent for most electrode materials [22], the parameter value used in this work is a constant for simplicity and for making a clear demonstration. It can be seen that the two methods can estimate the diffusion coefficient D_s successfully, with only small deviations from the value used in the model. Since the true value of D_s in the model, as well as other electrochemical parameters (see Table 1), are constant, ideally the estimated D_s value from the GITT and ICI methods should be a constant as well. However, as it is shown in Fig. 4a, the estimated D_s from the GITT and ICI methods has a significant dependence on the SOC. It can be observed that the trend of the estimated D_s in Fig. 4a has a good correlation with the dE/dx profile in Fig. 4b, and this is a hint that the deviations are related with the violation of one assumption in the mathematical derivation: *The voltage profile is linear during a short interval, i.e. dE/dc is a constant*. The true value of the dE/dx term is calculated from the open circuit voltage profile in (16). Although the SOC interval during a current pulse is relatively small (1.785% SOC change in a GITT current pulse), the minor variation in the dE/dx term cannot be ignored and its impact is directly reflected in the D_s estimation. This will be demonstrated in the next part. One more observation in Fig. 4b is that the GITT method can provide a better estimation of the dE/dx profile. This is expected, since in the GITT method, the dE/dx term is estimated between two equilibrium states and it is not affected by the current direction, taking into account that the open circuit voltage hysteresis is not included in the model. However, the ICI method obtains dE/dx during a galvanostatic charge and discharge, and therefore the estimation is slightly shifted depending on the current direction. As can be noted in Fig. 4a and b, in the beginning of the lithiation and delithiation processes in the ICI test, both the dE/dx term and the estimated D_s value have a larger mismatch from the true value, but the agreement improves with the time. Despite some minor shifts in the dE/dx estimation, the D_s value obtained from the ICI method has a very good agreement with those calculated using the GITT method.

4.2. Analysis of the deviations of D_s estimation

4.2.1. Non-linear voltage profile dE/dx

To demonstrate how the dE/dx term affects the D_s estimation, two cases at different SOC levels are studied in detail. In the first case ($x = 0.35$), dE/dx is changing rapid during the current pulse, while in the second case ($x = 0.8$) dE/dx is comparatively constant, which in turn fulfills the assumptions of the GITT derivation to a higher degree. Moreover, results with different fitting approaches and different fitting lengths are demonstrated as well. For the GITT method, the full expression fitting in (10) and with the $\tau \ll 1$ approximation fitting in (12) are applied with a fitting length varying from 20 s to 900 s. When it comes to the ICI method, the expression in (15) is used to find the diffusion coefficient, and the fitting length is from 1 s to 4 s. The voltage response in the first second is always excluded in the fitting to avoid the transient behaviours in other electrochemical processes in the system. The voltage response and its fitting are presented in Fig. 5 and the estimated

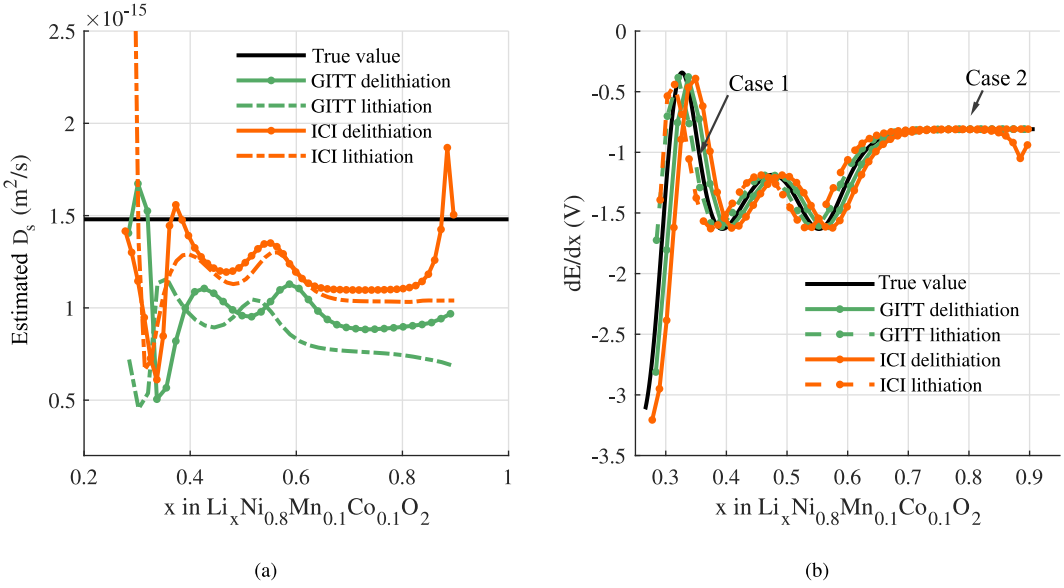

Fig. 4. (a) The derived diffusion coefficient D_s from the GITT and ICI simulations. (b) Estimated dE/dx from the GITT and ICI simulations.

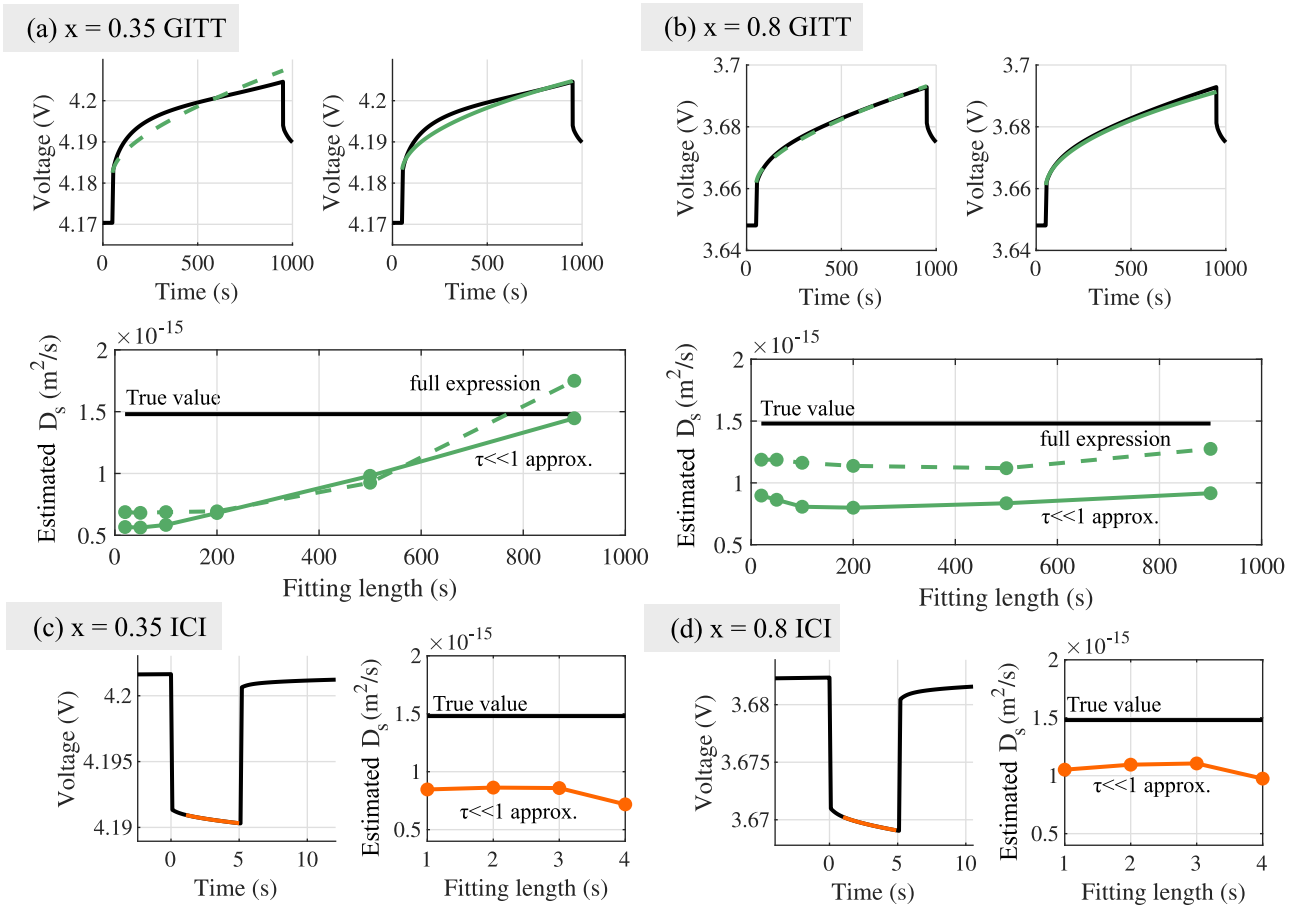

Fig. 5. The voltage response of $LiNi_{0.8}Mn_{0.1}Co_{0.1}O_2$ and its fitting to obtain its diffusion coefficient D_s in the GITT and ICI methods. The voltage response in black is the numerical solution simulated with a DFN model, and voltage response in colors are the analytical solutions with the fitted D_s, described in Eq. (10) as dashed line for the GITT method, (12) as the solid line for the GITT method and (15) as the solid line for the ICI method, respectively.

diffusion coefficient are compared with the true value used in the DFN model.

It can be observed that the analytical solutions of Fick's law (colored lines) cannot capture the voltage response accurately when $x = 0.35$ in Fig. 5a, due to the relatively large variation of the dE/dx term at this SOC level, as indicated in Fig. 4b. As a consequence, the estimated D_s when $x = 0.35$ has a larger deviation from the true value of 1.48×10^{-15} m^2/s, for both the full expression fitting (dashed lines) and $\tau \ll 1$ fitting (solid lines). It is seen in Fig. 5a that this estimation can be improved with a longer fitting length. On the other hand, the analytical solutions (colored lines) highly resemble the numerical solution with a DFN model (black lines) when $x = 0.8$ in Fig. 5b, since the voltage profile is more linear during the current pulse, i.e. the dE/dx term is close to a constant. Under these conditions, the estimated D_s is closer to the true value, especially using the full expression fitting. The validity of the $\tau \ll 1$ approximation was discussed in conjunction with Fig. 1, with the upper time axis calculated with the r_s and D_s values used in the model. The approximation is considered to be valid when $\tau < 0.0032$, i.e. $t < 58.92$ s. Therefore, the estimation discrepancy increases when the fitting length is increased from 20 s to 50 s and 100 s in Fig. 5b, as this approximation is losing its validity. When the fitting length is increased even longer, the overpotential contributions from the charge transfer reaction and electrolyte mass transportation plays a role in the fitting, causing an opposite effect to the invalidity of the $\tau \ll 1$ approximation, and improves the estimation in this case. Based on Fig. 5a and b, it can be concluded that the diffusion coefficient D_s can be estimated more accurately when the voltage profile is more linear. The same conclusion can be made with the ICI simulation results in Fig. 5c and d, that the estimated D_s with the ICI method is closer to the true value at $x = 0.8$ with a constant dE/dx. Moreover, it can be observed that in the ICI method, it is preferable to keep the fitting length short to better fulfill the $\tau \ll 1$ approximation. Despite the fact that the diffusion coefficient D_s is slightly underestimated in most of the presented cases, this is considered as a fairly accurate estimation, with the maximum error only being 66%.

4.2.2. Uneven current distribution through the porous electrode and overpotential

However, even when the voltage profile is linear at $x = 0.8$, it is still not possible to obtain exactly the true value of D_s irrespective of the fitting method and fitting length used. This can be explained with the violations of the other two assumptions in the derivation listed in the theory section: *The current density at the particle surface is constant* and *the over-potential caused by other electrochemical processes can be ignored*. To address these two issues, the current distribution in the electrode during one GITT pulse and the overpotential development are studied in detail in Fig. 6. In this analysis, the local current density and the overpotential at the particle closest to the current collector are studied, as it directly determines the measured terminal voltage. The current distribution during a current pulse in the GITT method at $x = 0.8$ is shown in Fig. 6a. When the current is applied at $t = 0$ s, the current density is higher at the separator side, since the electronic conductivity is much higher than the ionic conductivity and the current

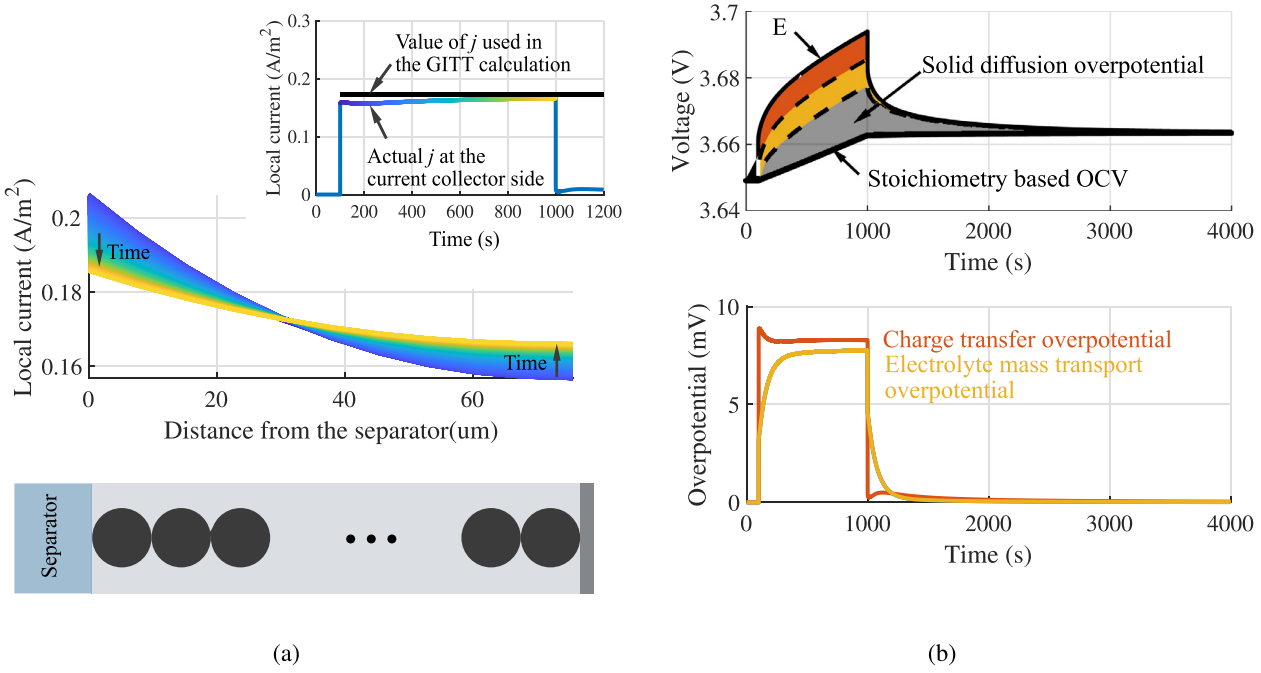

Fig. 6. During a current pulse at $x = 0.8$, (a) the current distribution in the electrode during one GITT pulse and (b) Overpotential at the current collector side.

tends to flow via the least resistive path. With time passing, the current density becomes more even through the porous electrode. The actual local current j at the current collector side is presented in Fig. 6a, and as can be seen, it is increasing with time. For the GITT fitting, the current is assumed to have an even distribution and the local current density j is estimated to be $j = I/(S_a L) = 0.17$ A/m^2 during a C/10 current pulse (plotted as the black line). It can be observed that in the beginning of the pulse, the actual current density at the current collector side is lower than 0.17 A/m^2, meaning that 0.17 A/m^2 is an overestimation of the local current density. This is one of the reasons for the disagreement between the estimated D_s value and the true value.

Besides the local current density, another factor causing this discrepancy is the overpotential caused by other electrochemical processes. As shown in Fig. 6b, the measurable voltage response E is the sum of the stoichiometry based voltage and the overpotential. In a DFN model, the overpotential is a consequence of three processes: the charge transfer reaction, electrolyte mass transport and the diffusion in the solid state. The charge transfer and solid diffusion overpotential are presented for the particle closest to the current collector, and the electrolyte mass transport overpotential is the difference between the electrolyte potential at the current collector point and electrolyte overpotential at the middle of the separator (the reference potential). Although it is only the solid diffusion overpotential that is the desired to use for the D_s estimation, in reality it is not possible to separate it from the other two overpotentials. It can be observed in Fig. 6b that both the charge transfer and electrolyte overpotential show a transient behaviour in the beginning of the pulse, which shall be avoided in the fitting. This is why the voltage response in the first second has been excluded in the previous demonstrations. These two overpotentials stabilize with time, and a higher electrolyte diffusion coefficient D_l and a faster reaction rate will speed up the stabilization. In the later part of the current pulse, these two overpotentials constitute an offset in the voltage response while the solid diffusion overpotential is still developing with time. This offset will still impact the fitting result as it introduces errors in the $dE/d\sqrt{t}$ fitting.

So far, the origins of the deviation of D_s estimation have been analysed and the difficulties in the estimation is found to be caused by the violations of the assumptions in the GITT method. This analysis and explanations are applicable also for other methods, for instance for PITT, which is derived based on similar assumptions as GITT.

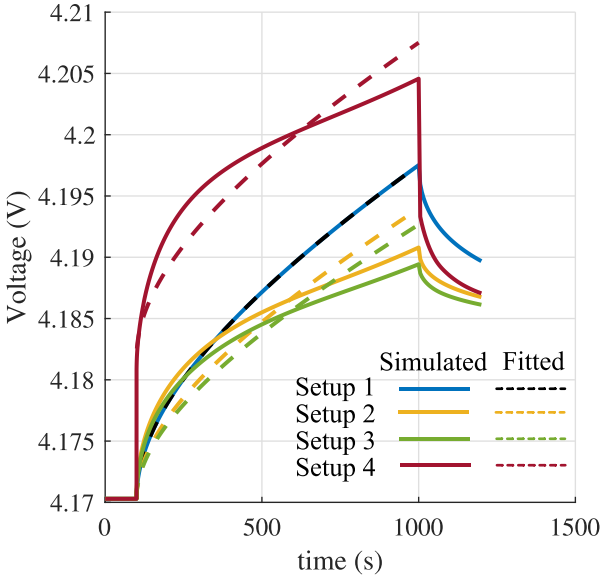

Fig. 7. The voltage response during a current pulse simulated with a black-box configured according to Table. 2 (solid lines) and its fitting with analytical expressions with (10) (dashed lines).

4.3. Special model setup with simplifications

To further demonstrate how the violations of the last three assumptions in the theory section can affect the result, four setups are studied, from the most simplified scenario to a more realistic system. Four black-box models are configured according to Table 2 and the simulated voltage responses are plotted as solid lines in Fig. 7. The simulated voltage response are then fitted with

Table 1
Parameters used in the simulation [7]. *Adjusted.*

Parameters	Values
L	75.6 μm
r_s	5.22 μm
ϵ_l	0.335
ϵ_s	0.665
Bruggeman constant	2.43
Open circuit voltage (OCV)	(16)
σ_s	10 S/m (original value 0.18 S/m)*
D_s	1.48×10^{-15} m^2/s
$c_{s,\max}$	51.77 mol/dm^3
$x_{\min}$ - $x_{\max}$	0.266-0.908
$k_a = k_c$	7×10^{-12} (original value 3.54×10^{-11})*
$\alpha_a = \alpha_c$	0.5
$c_{l,0}$	1 mol/dm^3
ϵ_l	0.47
D_l	1.77×10^{-10} m^2/s
κ	0.95 S/m
t_+^0	0.26
f_A	0

the analytical solutions, both with the full expression in (10), plotted as dashed lines, and the $\tau \ll 1$ approximation in (12), not shown in the figure. The first setup is an ideal scenario, where the voltage profile of the electrode material is perfectly linear, with a constant local current density and excluding the rest of the system. With this setup, the analytical solution of Fick's law can precisely represent the voltage response, as shown in Fig. 7, and the true D_s value can be accurately estimated without any deviations using the full expression fitting (10). However, the $\tau \ll 1$ fitting method leads to a 7.9% underestimation, since the approximation is conditionally valid. In the next setup, the voltage profile is a function of SOC, described in (16) at $x = 0.35$. The instant observation is that the analytical solution does not match the numerical solution anymore and the estimated D_s values differ more than 40% compared to the true value. To complicate the system further, an uneven current distribution in the electrode is included in Setup 3. With this more realistic current distribution, the local current density at the current collector side is lower than the average value, as demonstrated in Fig. 6a, and the voltage response in Setup 3 is therefore slightly lower than what is simulated with Setup 2. In the final setup, the overpotential caused by other electrochemical processes are included in the terminal voltage. This setup has the same condition as in a DFN model and the simulated voltage profile is identical to what was presented in Fig. 5a. Based on the fitting results in Table. 2, it can be noted that more violations of these assumptions do not necessarily lead to a worse estimation. The exact impact depends on the combination of the parameters in the system, as well as the current magnitude, which will be demonstrated in the next part.

4.4. Impact of electrolyte diffusion coefficient and current magnitude on D_s estimation

In the studies above, the estimation accuracy of D_s is affected by the fitting approach and fitting length. Besides, the battery design, current magnitude and the rest of the system can have a large impact on the results as well. To illustrate such effects, the result of the estimated D_s with a variation in the electrode thickness and current magnitude is presented in Fig. 8a. The scenario investigated is that a current pulse is applied at $t = 0$ s at $x = 0.8$, and the voltage response between $t = 1$ s and $t = 21$ s is used for fitting with the $\tau \ll 1$ approximation in (12). The same study is then performed when the diffusion coefficient in the electrolyte D_l in Table 1 is increased by 10 times; the results of this approach is shown in Fig. 8b. For both sets of parameters, the estimated value of D_s is higher when employing a thinner electrode and a higher current magnitude. With a 40 μm thick electrode and C/10 current, the estimated D_s is 32% lower than the true value in Fig. 8a, while the D_s estimation becomes only 5% lower than the true value in Fig. 8a, meaning that an increased electrolyte diffusion coefficient D_l can result in a higher estimation of the D_s value. This does not necessarily mean that this can improve the estimation, since it can lead to an overestimation under some conditions. When the GITT method is used for estimating lithium-ion battery aging, a decreasing trend in the D_s can be observed with the increase of the cycling numbers [11]. The result in Fig. 8 implies that apart from the active material degradation being the main reason, the decrease in D_s could also be partly due to the degradation of the electrolyte and a decreased D_l.

5. Conclusions

A theoretical validation of the GITT and ICI methods was demonstrated with a porous lithium-ion NMC811 electrode employing a DFN model. The deviations of the estimated D_s are explained with a focus on the violation of the assumptions in GITT, including the non-linear voltage profile, uneven current distribution in the porous electrode, as well as the overpotential caused by the charge transfer and electrolyte mass transport. Although the theoretical derivation of the GITT and ICI methods are based on multiple assumptions which are most likely not entirely valid for this type of lithium-ion battery electrode, both methods can still provide a very good estimation of the D_s value, with the maximum deviation being an underestimation of 66%. The estimation is more accurate when the voltage profile has a more linear shape, since the voltage response can then be better described with the analytical solution of Fick's law. For the GITT method, a longer fitting time can sometime provide a better estimation, while for the ICI method it is preferred to keep the fitting length short. With the parameter set used in this work, the solid-state diffusion coefficient is underestimated in most of the case. A higher current magnitude, a thinner electrode and a higher electrolyte diffusion coefficient can lead to a higher estimation for the D_s value, but can also render an overestimation. For the purpose of identifying the solid-state diffusion coefficient, the ICI method has a significant advantage of being time-effective. It should be acknowledged that GITT can be used to study also other properties of an electrode material, including the open circuit voltage and hysteresis. However, the ICI technique is much more convenient and powerful and it is suitable to be incorporated as part of a reference performance test for aging diagnostics.

Table 2
Four setups to investigate the impact of violations of assumptions.

	dE/dx	Local current	Overpotential caused by other processes	Fitted D_s with (12) between 1–20 s	Fitted D_s with (10) between 1–900 s
Setup 1	Constant	Constant	Excluded	1.36×10^{-15} m^2/s (-7.9%)	1.48×10^{-15} m^2/s (0%)
Setup 2	Varying	Constant	Excluded	0.85×10^{-15} m^2/s (-42.6%)	2.15×10^{-15} m^2/s (+45.3%)
Setup 3	Varying	Varying	Excluded	0.98×10^{-15} m^2/s (-33.6%)	2.53×10^{-15} m^2/s (+70.6%)
Setup 4 (DFN model)	Varying	Varying	Included	0.57×10^{-15} m^2/s (-61.7%)	1.73×10^{-15} m^2/s (+16.6%)

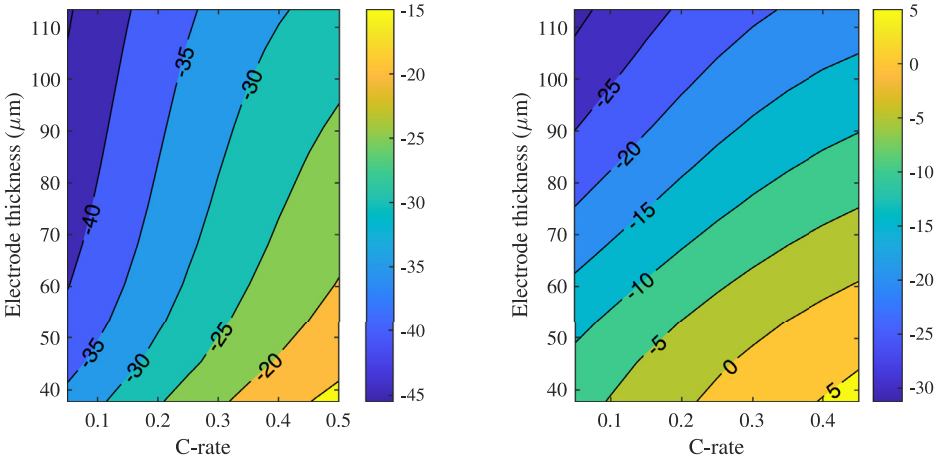

Fig. 8. The difference between the estimated D_s value and the true value with a variation in the electrode thickness and current magnitude with (a) the parameters listed in Table 1 (b) the diffusion coefficient in the electrolyte D_l is increased by 10 times.

Declaration of Competing Interest

The authors declare that they have no known competing financial interests or personal relationships that could have appeared to influence the work reported in this paper.

Credit authorship contribution statement

Zeyang Geng: Conceptualization, Methodology, Software, Validation, Writing – original draft, Visualization, Writing – review & editing. **Yu-Chuan Chien:** Conceptualization, Methodology, Writing – review & editing. **Matthew J. Lacey:** Conceptualization, Methodology, Writing – review & editing. **Torbjörn Thiringer:** Supervision, Funding acquisition, Writing – review & editing. **Daniel Brandell:** Supervision, Writing – original draft.

Acknowledgment

The authors would like to thank Energimyndigheten (P42789-1) for the financing of this work. Y.-C.C. and DB acknowledges STandUP for Energy.

Supplementary material

Supplementary material associated with this article can be found, in the online version, at 10.1016/j.electacta.2021.139727.

References

[1] J. Zheng, Z. Ren, P. Guo, L. Fang, J. Fan, Diffusion of Li+ ion on graphene: a DFT study, Appl. Surf. Sci. 258 (5) (2011) 1651–1655.
[2] G.K.P. Dathar, D. Sheppard, K.J. Stevenson, G. Henkelman, Calculations of Li-ion diffusion in olivine phosphates, Chem. Mater. 23 (17) (2011) 4032–4037.
[3] M.S. Islam, Ionic transport in ABO3 perovskite oxides: a computer modelling tour, J. Mater. Chem. 10 (4) (2000) 1027–1038.
[4] M.S. Islam, C.A. Fisher, Lithium and sodium battery cathode materials: computational insights into voltage, diffusion and nanostructural properties, Chem. Soc. Rev. 43 (1) (2014) 185–204.
[5] I. Santos-Mendoza, J. Vázquez-Arenas, I. González, G. Ramos-Sánchez, C. Castillo-Araiza, Revisiting electrochemical techniques to characterize the solid-state diffusion mechanism in lithium-ion batteries, Int. J. Chem. Reactor Eng. 17 (6) (2018).
[6] W. Weppner, R.A. Huggins, Determination of the kinetic parameters of mixed–conducting electrodes and application to the system Li_3Sb, J. Electrochem. Soc. 124 (10) (1977) 1569.
[7] C.-H. Chen, F.B. Planella, K. Oregan, D. Gastol, W.D. Widanage, E. Kendrick, Development of experimental techniques for parameterization of multi-scale lithium-ion battery models, J. Electrochem. Soc. 167 (8) (2020) 080534.
[8] A. Nickol, T. Schied, C. Heubner, M. Schneider, A. Michaelis, M. Bobeth, G. Cuniberti, GITT analysis of lithium insertion cathodes for determining the lithium diffusion coefficient at low temperature: challenges and pitfalls, J. Electrochem. Soc. 167 (9) (2020) 090546.
[9] D.W. Dees, S. Kawauchi, D.P. Abraham, J. Prakash, Analysis of the galvanostatic intermittent titration technique (GITT) as applied to a lithium-ion porous electrode, J. Power Sources 189 (1) (2009) 263–268.
[10] M.J. Lacey, Influence of the electrolyte on the internal resistance of lithium- sulfur batteries studied with an intermittent current interruption method, ChemElectroChem 4 (8) (2017) 1997–2004.
[11] Y.-C. Chien, H. Liu, A.S. Menon, W.R. Brant, D. Brandell, M.J. Lacey, A fast alternative to the galvanostatic intermittent titration technique (2021). doi:10.33774/chemrxiv-2021-09srz.
[12] C. Deng, W. Lu, Consistent diffusivity measurement between galvanostatic intermittent titration technique and electrochemical impedance spectroscopy, J. Power Sources 473 (2020) 228613.
[13] S. Liu, An analytical solution to li/li+ insertion into a porous electrode, Solid State Ionics 177 (1–2) (2006) 53–58.
[14] N. Garcia-Araez, J.W. Dibden, N. Meddings, J. Owen, Quantitative galvanostatic intermittent titration technique for the analysis of a model system with applications in lithium- sulfur batteries, ChemElectroChem 5 (3) (2018) 445–454.
[15] M. Doyle, T.F. Fuller, J. Newman, Modeling of galvanostatic charge and discharge of the lithium/polymer/insertion cell, J. Electrochem. Soc. 140 (6) (1993) 1526.
[16] T.F. Fuller, M. Doyle, J. Newman, Simulation and optimization of the dual lithium ion insertion cell, J. Electrochem. Soc. 141 (1) (1994) 1–10.
[17] Z. Geng, S. Wang, M.J. Lacey, D. Brandell, T. Thiringer, Bridging physics-based and equivalent circuit models for lithium-ion batteries, Electrochim. Acta 372 (2021) 137829.
[18] J. Sturm, A. Rheinfeld, I. Zilberman, F.B. Spingler, S. Kosch, F. Frie, A. Jossen, Modeling and simulation of inhomogeneities in a 18650 nickel-rich, silicon–graphite lithium-ion cell during fast charging, J. Power Sources 412 (2019) 204–223.
[19] C. Delacourt, M. Ati, J. Tarascon, Measurement of lithium diffusion coefficient in Li y FeSO4F, J. Electrochem. Soc. 158 (6) (2011) A741.
[20] Y. Wei, J. Zheng, S. Cui, X. Song, Y. Su, W. Deng, Z. Wu, X. Wang, W. Wang, M. Rao, et al., Kinetics tuning of Li-ion diffusion in layered Li (Ni x Mn y Co z) O2, J. Am. Chem. Soc. 137 (26) (2015) 8364–8367.
[21] Z. Shen, L. Cao, C.D. Rahn, C.-Y. Wang, Least squares galvanostatic intermittent titration technique (LS-GITT) for accurate solid phase diffusivity measurement, J. Electrochem. Soc. 160 (10) (2013) A1842.
[22] K. Persson, V.A. Sethuraman, L.J. Hardwick, Y. Hinuma, Y.S. Meng, A. Van Der Ven, V. Srinivasan, R. Kostecki, G. Ceder, Lithium diffusion in graphitic carbon, J. Phys. Chem. Lett. 1 (8) (2010) 1176–1180.